Machine Learning Based Power Control for a Secondary Cell-Free Network

Rimalapudi Sarvendranath, *Member, IEEE*, Kalpeswar Paul.

2023 National Conference on Communications (NCC) | 978-1-6654-5625-8/23/$31.00 ©2023 IEEE | DOI: 10.1109/NCC56989.2023.10067923

***Abstract*—Cell-free networks, in which a large number of distributed antennas transmit high speed data to multiple users, is emerging as a next generation wireless technology. Cell-free networks that share spectrum in an underlay manner provides above benefits and improves the utilization of the crowded spectrum. We focus on a well motivated problem of optimal power allocation to maximize the energy efficiency (EE) of an underlay cell-free network. This forms a non-convex optimization problem, which is computationally complex to solve. To reduce this complexity, in this work, we develop different machine learning models that can estimate the power allocation coefficients. We develop two deep neural network models and a decision tree model. Training data is generated with multiple practical limitations such as imperfect channel state information and spatial channel correlation. Our simulations show that these machine learning models perform very close to the traditional optimization techniques.**

***Index Terms*—Cell-free, spectrum sharing, energy efficiency, power control, machine learning, deep neural network.**

I. Introduction

Cell-free massive multiple-input-multiple-output (MIMO) is an emerging technology built on the time division duplex (TDD) mode of massive MIMO operation. In it, distributed access points (AP) jointly transmit data to the users in an user-centric manner [1]. These distributed APs are coordinated by a central entity referred as central processing unit (CPU). This distributed architecture with large number of transmit antennas at different geographical locations provide several benefits. It provides robustness to signal blockages as the chances of user-equipment (UE) being close to some of the antennas increase. Also provides better path loss conditions [2].

Spectrum sharing is yet another crucial technique required to enable next generation wireless technologies such as cell-free massive MIMO. This is due to over crowding of the wireless spectrum with existing technologies especially in lower frequencies with good propagation characteristics. Thus designing a cell-free network that shares spectrum with existing technologies enables us to provide high speed data services to large number of UEs within the available scarce wireless spectrum [3]–[5].

Given the importance of spectrum sharing, it has been incorporated in to long term evolution (LTE) and 5G new radio unlicensed. It is also part of the WiFi standards such as IEEE 802.11be [6] and other wireless standards such as MulteFire and Citizen's broadband radio service. Even the spectrum regulators around the world have accepted the need for spectrum sharing. Federal Communications Commission has opened spectrum in 3 GHz and 6 GHz bands for shared and unlicensed operations [7], [8]. Some of these bands are open for low-power indoor operations. We focus on the underlay mode of the spectrum sharing, in which a secondary system, who may not own the license to the spectrum, transmits simultaneously with the primary system with spectrum usage license [3], [9]. Hence, the secondary system causes interference to the primary system and is subject to the interference constraints.

Traditional Techniques: Underlay cell-free systems have been widely studied with traditional optimization based techniques. In [3], a power allocation policy is developed under minimum signal-interference-noise-ratio (SINR) constraint at primary and secondary systems. A sum-rate maximization problem is studied in [4] for an underlay cell-free massive MIMO system sharing spectrum with a primary massive MIMO system. The *energy efficiency (EE)*, which is equal to the number of bits communicated per unit energy, maximization of a cell-free massive MIMO was studied in [10], [11]. A downlink power allocation policy is developed in [11] for a cell-free massive MIMO system with maximal-ratio (MR) precoding under the assumption of uncorrelated channels. A Dinkelbach's algorithm based iterative power allocation procedure is developed to maximize the EE of any underlay cell-free network in [12]. It is shown to improve EE significantly compared to the simpler equal power allocation scheme.

Machine Learning Techniques: A deep learning based power allocation is studied in massive MIMO [13]. A fully-connected feedforward deep neural network (DNN) is trained to take UE locations as inputs and output the optimal power allocation. A convolutional layer based DNN is constructed to estimate the max-min power allocation for a cell-free massive MIMO system in [14]. It is shown to provide a good approximation with significantly lower complexity. An unsupervised learning based DNN that learns optimal UE power allocations to maximize the minimum user rate is proposed in [15]. A deep learning based distributed power allocation scheme that uses only the information available at each AP is developed in [16]. A DNN that improves the spectral efficiency (SE) of a heuristic power allocation scheme is developed based on the large-scale fading parameters. However, to the best of our knowledge, the performance of the machine learning techniques is not studied for an underlay cell-free network.

Focus and Contributions: Our work focuses on well motivated problem of EE maximization, which is crucial for an

Rimalapudi Sarvendranath is with the Department of Electronics and Electrical Engineering, Indian Institute of Technology, Guwahati and Kalpeswar Paul is with Department of Electronics and Telecommunication Engineering, Assam Engineering College, Guwahati. Emails: sarvendranath@iitg.ac.in, kalpeswar11@gmail.com.

Authorized licensed use limited to: INDIAN INSTITUTE OF TECHNOLOGY GUWAHATI. Downloaded on June 06,2023 at 07:45:14 UTC from IEEE Xplore. Restrictions apply.

underlay cell-free system for better use of the energy. We consider an underlay cell-free system, in which multiple APs communicates to secondary UEs in a centralized manner. It transmits simultaneously in the same spectrum as a primary massive MIMO system. We consider multiple practical assumptions as follows: (i) Secondary APs perform precoding only based on the estimated channel gains, which is different from more widely considered perfect CSI. (ii) Channel gains at each secondary AP are considered to be correlated rather than simpler independent assumption. (iii) Only channel statistics are assumed at the CPU to compute power allocation coefficients. This reduces the amount of information that needs to be transmitted between APs and CPU. This is because the channel statistics vary at a slower pace compared to the instantaneous channel gains. (iv) The average interference constraint considered is more practical than the instantaneous interference constraints and works even with imperfect CSI [3], [17] .

We develop different machine learning models that estimate the optimal power allocation coefficients, which maximize the EE of an underlay cell-free system subject to a peak transmit power constraint at each secondary AP and an average interference constraint at each primary UE. We develop two DNN models, which approximate the optimal EE power allocation with much lower complexity than the traditional optimization techniques. Our numerical results show that both DNN models perform close to the traditional optimization techniques and model 1 does it with a small number of trainable parameters. We also develop a decision tree based machine learning model whose performance matches exactly with the optimization methods.

Notations: The absolute value of a scalar b is denoted by $\|b\|$, Column vectors $\mathbf{a}$ are denoted by boldface lowercase letters and their l_2 norm is denoted by $|\mathbf{a}|$. The matrices are denoted by boldface uppercase letters. $\mathbf{I}_N$ denotes the $N \times N$ identity matrix. Conjugate, transpose, and Hermitian transpose are denoted by the superscripts $(\cdot)^*$, $(\cdot)^T$, and $(\cdot)^H$, respectively. $\mathbb{E}\{X\}$ denotes the expected value of a random variable X. A circular symmetric complex Gaussian random vector $\mathbf{z}$ is denoted by $\mathbf{z} \sim \mathcal{CN}(\mathbf{0}, \mathbf{R})$, where $\mathbf{R}$ is its covariance matrix.

II. Underlay Cell-Free Massive MIMO System

We consider a single cell downlink secondary cell-free network that shares spectrum with a primary massive MIMO system in an underlay manner. The primary Massive MIMO basestation (BS) with M collocated antennas communicates to K_{p} single-antenna primary UEs [3]. our system model is shown in Fig. 1. The secondary cell-free network has L APs serving K_{s} single-antenna UEs. Each secondary AP has N antennas.

Let $\mathbf{h}_{kl}$, $\mathbf{f}_{\text{sp-}ml}$, $\mathbf{f}_{\text{ps-}i}$ and $\mathbf{g}_m$ be the channel gains from the l^{th} secondary AP to k^{th} secondary UE, l^{th} secondary AP to m^{th} primary UE, from primary BS to i^{th} secondary UE, and primary BS to m^{th} primary UE, respectively. Let $\mathbf{R}_{kl} \in \mathbb{C}^{N\times N}$, $\mathbf{F}_{\text{sp-}ml} \in \mathbb{C}^{N\times N}$, $\mathbf{F}_{\text{ps-}i} \in \mathbb{C}^{M\times M}$ and $\mathbf{G}_m \in \mathbb{C}^{M\times M}$ denote corresponding correlation matrices, which are known to the

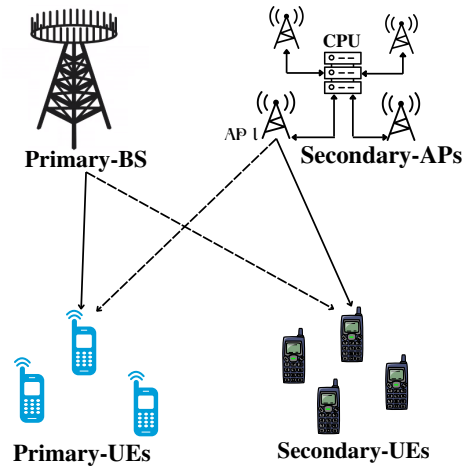


Fig. 1: An underlay cell free network coexisting with a massive MIMO primary system.

secondary APs and the CPU. We assume that $\mathbf{h}_{kl}$, $\mathbf{f}_{\text{sp-}ml}$, $\mathbf{f}_{\text{ps-}i}$ and $\mathbf{g}_i$ are mutually independent. Correlated Rayleigh fading has been considered. Therefore, $\mathbf{h}_{kl} \sim \mathcal{CN}(\mathbf{0}, \mathbf{R}_{kl})$, $\mathbf{f}_{\text{sp-}ml} \sim \mathcal{CN}(\mathbf{0}, \mathbf{F}_{\text{sp-}ml})$, $\mathbf{f}_{\text{ps-}i} \sim \mathcal{CN}(\mathbf{0}, \mathbf{F}_{\text{ps-}i})$ and $\mathbf{g}_m \sim \mathcal{CN}(\mathbf{0}, \mathbf{G}_m)$. The secondary UEs know only the channel statistics.

A. Channel Estimation

The primary and secondary systems operate in synchronous TDD mode and both systems perform uplink and downlink operations simultaneously. Therefore, assuming reciprocity, pilots sent by the UEs in uplink are used to estimate the downlink channel gains. The length of the coherence interval and the length of the pilot sequence are denoted by τ_{c} and $\tau_{\mathrm{p}} \leq \tau_{\mathrm{c}}$, respectively. Let $\mathbf{\Phi} = [\boldsymbol{\phi}_1, \ldots, \boldsymbol{\phi}_{\mathrm{p}}] \in \mathbb{C}^{\tau_{\mathrm{p}}\times\tau_{\mathrm{p}}}$ denote the collection of τ_{p} mutually orthogonal pilot sequences. Let $\|\boldsymbol{\phi}_k\| = 1$, for $k = 1, \ldots, \tau_{\mathrm{p}}$. We split these τ_{p} pilot sequences into two groups with τ_1 and τ_2 pilot sequences such that $\tau_1 + \tau_2 = \tau_{\mathrm{p}}$. These are denoted by $\mathbf{\Phi}_{\mathrm{p}} \in \mathbb{C}^{\tau_{\mathrm{p}}\times\tau_2}$, and $\mathbf{\Phi}_{\mathrm{s}} \in \mathbb{C}^{\tau_{\mathrm{p}}\times\tau_1}$. Here, $\mathbf{\Phi}_{\mathrm{p}}$ and $\mathbf{\Phi}_{\mathrm{s}}$ contain the pilot sequences allocated to primary and secondary systems, respectively. Let $\mathbf{\Phi} = [\mathbf{\Phi}_{\mathrm{p}}, \mathbf{\Phi}_{\mathrm{s}}]$.

The index of the pilot sequence transmitted by the k^{th} secondary UE is denoted by t_k and $\mathcal{S}_k$ denotes the set of secondary UEs that use pilot sequence $\boldsymbol{\phi}_{t_k}$. Let $\widehat{\mathbf{h}}_{kl}$ denote the minimum-mean square error (MMSE) estimate of $\mathbf{h}_{kl}$. When the secondary UEs and primary UEs transmit the pilot sequences with powers η_{s} and η_{p}, respectively, the l^{th} secondary AP receives

$$\mathbf{Y}_l^{\mathrm{p}} = \sqrt{\eta_{\mathrm{s}}} \sum_{i=1}^{K_{\mathrm{s}}} \mathbf{h}_{il} \boldsymbol{\phi}_{t_i}^T + \sqrt{\eta_{\mathrm{p}}} \sum_{j=1}^{K_{\mathrm{p}}} \mathbf{f}_{\text{sp-}jl} \boldsymbol{\phi}_{t_j}^T + \mathbf{N}_l, \quad (1)$$

where $\mathbf{N}_l \in \mathbb{C}^{N\times\tau_{\mathrm{p}}}$ is the additive white Gaussian noise. Each element of $\mathbf{N}_l$ is independent and identically distributed circular symmetric complex Gaussian random variables with variance σ^2.

Authorized licensed use limited to: INDIAN INSTITUTE OF TECHNOLOGY GUWAHATI. Downloaded on June 06,2023 at 07:45:14 UTC from IEEE Xplore. Restrictions apply.

To obtain the channel estimate $\widehat{\mathbf{h}}_{kl}$, we first project $\mathbf{Y}_l^{\mathrm{p}}$ on $\boldsymbol{\phi}_{t_k}$, which is given by

$$\mathbf{y}_{t_k l}^{\mathrm{p}} = \mathbf{Y}_l^{\mathrm{p}} \boldsymbol{\phi}_{t_k}^* = \sqrt{\eta_{\mathrm{s}}} \sum_{i \in \mathcal{S}_k} \mathbf{h}_{il} + \mathbf{n}_{t_k l}, \tag{2}$$

where $\mathbf{n}_{t_k l} = \mathbf{N}_l \boldsymbol{\phi}_{t_k}^* \sim \mathcal{CN}(\mathbf{0}, \sigma^2 \mathbf{I}_N)$. The MMSE estimate $\widehat{\mathbf{h}}_{kl}$ as a function of $\mathbf{y}_{t_k l}^{\mathrm{p}}$ is given by

$$\widehat{\mathbf{h}}_{kl} = \sqrt{\eta_{\mathrm{s}}} \mathbf{R}_{kl} \boldsymbol{\Psi}_{t_k l}^{-1} \mathbf{y}_{t_k l}^{\mathrm{p}}, \tag{3}$$

where

$$\boldsymbol{\Psi}_{t_k l} = \eta_{\mathrm{s}} \sum_{i \in \mathcal{S}_k} \mathbf{R}_{il} + \sigma^2 \mathbf{I}_N. \tag{4}$$

Let $\widetilde{\mathbf{h}}_{kl} = \mathbf{h}_{kl} - \widehat{\mathbf{h}}_{kl}$ denote the error. On simplification we can show that $\widehat{\mathbf{h}}_{kl} \sim \mathcal{CN}(\mathbf{0}, \eta_{\mathrm{s}} \mathbf{R}_{kl} \boldsymbol{\Psi}_{t_k l}^{-1} \mathbf{R}_{kl})$ and the estimation error $\widetilde{\mathbf{h}}_{kl} \sim \mathcal{CN}(\mathbf{0}, \mathbf{R}_{kl} - \eta_{\mathrm{s}} \mathbf{R}_{kl} \boldsymbol{\Psi}_{t_k l}^{-1} \mathbf{R}_{kl})$. Let $\widehat{\mathbf{R}}_{kl} = \eta_{\mathrm{s}} \mathbf{R}_{kl} \boldsymbol{\Psi}_{t_k l}^{-1} \mathbf{R}_{kl}$ and $\widetilde{\mathbf{R}}_{kl} = \mathbf{R}_{kl} - \widehat{\mathbf{R}}_{kl}$.

B. Transmit Beamforming and Downlink Transmission

Let $\mathbf{w}_{il}$ denote the precoding vector employed by the l^{th} secondary AP to transmit data symbol d_i ($\mathbb{E}\{|d_i|^2\} = 1$) to the i^{th} secondary UE. Each secondary AP performs MR precoding based on the channel estimates obtained as follows [18]

$$\mathbf{w}_{il} = \frac{\widehat{\mathbf{h}}_{il}}{\sqrt{\mathbb{E}\{\|\widehat{\mathbf{h}}_{il}\|^2\}}}, \tag{5}$$

Let $p_{il} \geq 0$ denote the transmit power allocated by the l^{th} secondary AP to the i^{th} secondary UE. Therefore, the signal $\mathbf{x}_l$ transmitted by the l^{th} secondary AP is given by

$$\mathbf{x}_l = \sum_{i=1}^{K_{\mathrm{s}}} \sqrt{p_{il}} \mathbf{w}_{il} d_i, \quad l = 1, \ldots, L. \tag{6}$$

Let $\bar{\mathbf{x}}_p$ and $\mathbf{Q}_p = \mathbb{E}\{\bar{\mathbf{x}}_p \bar{\mathbf{x}}_p^H\}$ denote the primary transmit signal and its correlation matrix, respectively. Then, the k^{th} secondary UE receives

$$\begin{aligned} y_k &= \sum_{l=1}^{L} \mathbf{h}_{kl}^H \mathbf{x}_l + \mathbf{f}_{\text{ps-}k}^H \bar{\mathbf{x}}_p + n_k, & (7)\\ &= \sum_{l=1}^{L} \sqrt{p_{kl}} \mathbf{h}_{kl}^H \mathbf{w}_{kl} q_k + \sum_{\substack{i=1 \\ i \neq k}}^{K_{\mathrm{s}}} \sum_{l=1}^{L} \sqrt{p_{il}} \mathbf{h}_{kl}^H \mathbf{w}_{il} d_i & (8)\\ &\quad + \mathbf{f}_{\text{ps-}k}^H \bar{\mathbf{x}}_p + n_k, \end{aligned}$$

where $n_k \sim \mathcal{CN}(0, \sigma^2)$ is the additive white Gaussian noise at the k^{th} secondary UE.

The secondary UE k only knows $\mathbb{E}\{\mathbf{h}_{kl}^H \mathbf{w}_{kl}\}$, for $l = 1, \ldots, L$. Therefore, adding and subtracting $\sum_{l=1}^{L} \sqrt{p_{kl}} \mathbb{E}\{\mathbf{h}_{kl}^H \mathbf{w}_{kl}\} q_k$ to y_k in (7), we get

$$\begin{aligned} y_k = &\sum_{l=1}^{L} \sqrt{p_{kl}} \mathbb{E}\{\mathbf{h}_{kl}^H \mathbf{w}_{kl}\} q_k \\ &+ \sum_{l=1}^{L} \sqrt{p_{kl}} \left(\mathbf{h}_{kl}^H \mathbf{w}_{kl} - \mathbb{E}\{\mathbf{h}_{kl}^H \mathbf{w}_{kl}\}\right) q_k \\ &+ \sum_{\substack{i=1 \\ i \neq k}}^{K_{\mathrm{s}}} \sum_{l=1}^{L} \sqrt{p_{il}} \mathbf{h}_{kl}^H \mathbf{w}_{il} d_i + d_k + n_k \end{aligned} \tag{9}$$

The, use-and-forget bound on SE achieved by k^{th} UE can be written as [19]

$$\mathrm{SE}_k = \left(1 - \frac{\tau_p}{\tau_c}\right) \log_2(1 + \Gamma_k) \ \text{bit/s/Hz}, \tag{10}$$

where the effective SINR Γ_k is derived in [12], [18]. It is given by [12, (13)]

$$\Gamma_k = \frac{\left(\sum_{l=1}^{L} \sqrt{p_{kl}} a_{kkl}\right)^2}{\sum_{l=1}^{L} \sum_{i=1}^{K_{\mathrm{s}}} p_{il} b_{ikl} + \sum_{i=1, i \neq k}^{K_{\mathrm{s}}} \left(\sum_{l=1}^{L} \sqrt{p_{il}} a_{ikl}\right)^2 + \sigma_k^2}, \tag{11}$$

where

$$b_{ikl} = \frac{\mathrm{Tr}(\mathbf{R}_{il} \boldsymbol{\Psi}_{t_i l}^{-1} \mathbf{R}_{il} \mathbf{R}_{kl})}{\mathrm{Tr}(\mathbf{R}_{il} \boldsymbol{\Psi}_{t_i l}^{-1} \mathbf{R}_{il})}, \tag{12a}$$

$$a_{ikl} = \mathbb{I}_{\mathcal{S}_k}(i) \frac{\eta_{\mathrm{s}} \tau_{\mathrm{p}} \mathrm{Tr}(\mathbf{R}_{il} \boldsymbol{\Psi}_{t_i l}^{-1} \mathbf{R}_{kl})}{\sqrt{\eta_{\mathrm{s}} \tau_{\mathrm{p}} \mathbf{R}_{il} \boldsymbol{\Psi}_{t_i l}^{-1} \mathbf{R}_{il}}}, \tag{12b}$$

where $\sigma_k^2 = \mathrm{Tr}(\mathbf{Q}_p \mathbf{F}_{\text{ps-}k}) + \sigma^2$. Here, $\mathbb{I}_{\mathcal{S}_k}(i)$ is 1 if the secondary UE i transmits $\boldsymbol{\phi}_{t_k}$ and 0 otherwise.

III. Energy Efficiency and Problem Statement

Let $\mathbf{p} = [p_{11}, \ldots, p_{K_{\mathrm{s}}1}, \ldots, p_{1L}, \ldots, p_{K_{\mathrm{s}}L}]^T$ be a concatenated vector of length $K_{\mathrm{s}} L$ with all power coefficients and $\mathrm{P_c}$ denote the total circuit power consumed at all the secondary APs. Therefore, the total power consumed, which we denote by $P_T(\mathbf{p})$, in the secondary system is given by

$$P_T(\mathbf{p}) = \sum_{i=1}^{K_{\mathrm{s}}} \sum_{l=1}^{L} p_{il}/\eta + \mathrm{P_c}, \tag{13}$$

where η denotes the efficiency of the power amplifier.

Energy Efficiency: of the cell-free network is defined as the ratio between the throughput summed over all the users to the total power consumed. It is given by

$$\mathrm{EE}(\mathbf{p}) = \frac{\sum_{k=1}^{K_{\mathrm{s}}} B \cdot \mathrm{SE}_k(\mathbf{p})}{P_T(\mathbf{p})}, \tag{14}$$

where B is the bandwidth of the secondary system.

We now introduce the two constraints imposed on the secondary system:

Authorized licensed use limited to: INDIAN INSTITUTE OF TECHNOLOGY GUWAHATI. Downloaded on June 06,2023 at 07:45:14 UTC from IEEE Xplore. Restrictions apply.

- *Peak Transmit Power Constraint*: It constrains the total transmit power at each secondary AP, i.e., $\sum_{i=1}^{K_\mathrm{s}} p_{il}$, to be below $P_{\max}$, which is the maximum transmit power allowed. It is given by

$$\sum_{i=1}^{K_\mathrm{s}} p_{il} \leq P_{\max},\ l = 1, \cdots, L. \tag{15}$$

- *Average Interference Power Constraint [3], [17]*: The instantaneous interference seen by m^{th} primary UE is given by

$$y_m^{'} = \sum_{l=1}^{L} \mathbf{f}_{\text{sp-}ml}^{H} \mathbf{x}_l. \tag{16}$$

The average interference power received at m^{th} primary UE can be obtained by averaging $|\mathbf{y}_m^{'}|^2$. It is given by

$$\mathbb{E}\{|\mathbf{y}_m^{'}|^2\} = \sum_{i=1}^{K_\mathrm{s}} \sum_{l=1}^{L} p_{il} \vartheta_{iml}, \tag{17}$$

where

$$\vartheta_{iml} = \mathrm{Tr}(\widehat{\mathbf{R}}_{il} \mathbf{F}_{\text{sp-}ml}) / \mathrm{Tr}(\widehat{\mathbf{R}}_{il}). \tag{18}$$

This constraint mandates that the average interference power at the primary UE should not exceed $\mathcal{I}_{\mathrm{th}}$ i.e., $\mathbb{E}\{|\mathbf{y}_m^{'}|^2\} \leq \mathcal{I}_{\mathrm{th}}$.

Our problem of developing optimal downlink power allocation to maximize the EE of an underlay cell-free network subject to above two constraints can be written as:

$$\mathcal{P}: \quad \max_{\mathbf{p}} \quad \frac{\sum_{k=1}^{K_\mathrm{s}} B \cdot \mathrm{SE}_k(\mathbf{p})}{\overline{P}_T(\mathbf{p})}, \tag{19a}$$

$$\text{s.t.} \quad \sum_{i=1}^{K_\mathrm{s}} p_{il} \leq P_{\max},\ l = 1, \ldots, L, \tag{19b}$$

$$p_{il} \geq 0,\ i = 1, \ldots, K_\mathrm{s};\ l = 1, \ldots, L. \tag{19c}$$

$$\sum_{l=1}^{L} \sum_{i=1}^{K_\mathrm{s}} p_{il} \vartheta_{iml} \leq \mathcal{I}_{\mathrm{th}},\ m = 1, \ldots, K_\mathrm{p} \tag{19d}$$

In the above optimization problem the constraints are convex. However, the optimization problem $\mathcal{P}$ is non-convex as the EE is non-convex. It can be solved by developing a convex lower bound of the objective function by writing the numerator of the EE as difference two logarithmic terms, which are concave functions of the power coefficients. As shown in [12], the second term in the difference can be upper bounded using first order Taylor series expansion. Substituting this in the numerator of the EE yields a concave lower bound. Therefore, the modified objective function becomes a ratio of a concave function and a linear function. We can solve this modified problem using Dinkelbach's algorithm as shown in [12].

IV. Machine Learning Based Power Allocation

We now develop different machine learning models for the energy efficient power allocation of an underlay cell-free network. First, we explain the generation of the training dataset and then briefly describe the deep learning and decision trees.

A. Dataset Generation

We first fix the locations of the primary BS and the secondary APs and follow the below steps to generate dataset:

1) Randomly drop the secondary UEs and primary UEs.
2) Compute the channel correlation matrices.
3) Compute a_{ikl}, b_{ikl}, ϑ_{iml}.
4) Solve the optimization problem $\mathcal{P}$ using the Dinkelbach's algorithm and obtain the optimal power allocation vector $\mathbf{P}^*$ [12].
5) **Input:** Concatenate all the values of a_{ikl}, b_{ikl}, ϑ_{iml} into one vector, which forms the input of the training dataset. Here, input vector is of length $K_\mathrm{s} L\,(1 + K_\mathrm{s} + K_\mathrm{p})$
6) **Output:** Optimal power allocation vector $\mathbf{P}^*$ of length $K_\mathrm{s} L$ forms the output vector corresponding to the input.

The above steps 1 to 6 are repeated N_{ds} times to generate the complete dataset.

B. Deep learning

First, we exploit the universal function approximation power of the neural networks to train a DNN that estimates the optimal power allocation with lower computational complexity [20]. Specifically, we employ a fully connected feedforward neural network with input layer of size $K_\mathrm{s} L\,(1 + K_\mathrm{s} + K_\mathrm{p})$. The output layer is of the dimension $K_\mathrm{s} L$ to estimate the optimal power allocation vector. Let $\hat{\mathbf{P}} \in \mathrm{R}_{+}^{K_\mathrm{s} L}$ denote the estimated power vector. Now training the DNN requires obtaining weights and bias terms so the estimated power is close to the optimal power obtained through traditional optimization algorithm. They are obtained by minimizing a loss function that is function of the optimal power allocation vector $\mathbf{P}^*$ and the estimated power vector $\hat{\mathbf{P}}$. Once we obtain these weights and biases the DNN can estimate the optimal power allocation vector for test vectors that were not used during training. Therefore, the power allocation can be obtained by feeding the new channel statistics to the DNN without having to solve the complex optimization algorithm.

C. Decision Trees

We now look at decision trees, which are widely used for multi-class classification, regression and clustering, to exploit their faster training and evaluation capability. We focus on binary decision trees in which each parent node has maximum two child nodes. Decision trees are formed by defining questions on the input features at each node. Each training sample is passed through these questions and placed at the leaf nodes depending on the questions formed in the tree and its structure. The greedy algorithm to form a decision tree that partitions the dataset is given in [21, Sec. 8.3.3]. Forming a decision tree with complex questions will form better partitions at the cost of increased complexity.

Partitioning: The training data is partitioned by passing each sample of the training set through the tree by answering questions at each node. We move to the right child when answer is positive and to the left child if the answer is negative. This process is continued till we reach a leaf node. All the samples that reach one leaf node forms a partition. *Estimation:*

Authorized licensed use limited to: INDIAN INSTITUTE OF TECHNOLOGY GUWAHATI. Downloaded on June 06,2023 at 07:45:14 UTC from IEEE Xplore. Restrictions apply.

Table I: Secondary and primary networks considered for performance comparison.

Secondary network	
Room size	$125\ \text{m} \times 125\ \text{m}$
Secondary APs	$L = 6$
Antennas at each AP	$N = 4$
Uniform linear array	Half-wavelength spacing
Spatial correlation	Local scattering model
Secondary UEs	$K_{\text{s}} = 4$
Primary network	
Primary cell area	$100\ \text{m} \times 100\ \text{m}$
Antennas at the BS	$M = 5$
Primary UEs	$K_{\text{p}} = 4$

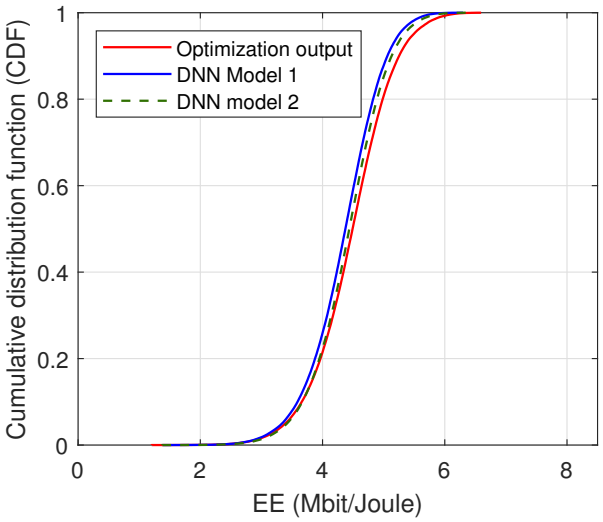


Fig. 2: Performance comparison of DNN models with the traditional optimization output.

To estimate the output of a test sample, we do the same process as partitioning. We pass the features of the test sample through the tree till we reach the leaf node. The estimated value of this test sample is equal to the average of output of all the training samples that fall under the leaf node.

V. Performance Comparison

We now compare the performance of the DNN and decision tree based regression models with the output of the traditional optimization algorithm. We consider an indoor secondary cell-free network with APs spaced on walls sharing spectrum with an outdoor massive MIMO system. The primary and secondary system parameters considered are in Table I. Both secondary UEs and primary UEs are distributed uniformly.

The large-scale fading due to path-loss is modeled as $-30.5 + 36.7 \log_{10}(\text{d})$ dB, where d is the distance from the transmitter to the receiver. The noise variance $\sigma^2 = -92$ dBm. We consider $\tau_{\text{c}} = 2000$, $\tau_{\text{p}} = 8$, $\eta = 0.35$, and $\text{P}_{\text{c}} = 1$ W. We assume that the interference from the primary BS to the secondary UEs is negligible due to favorable propagation effect of the massive MIMO.

We generated a dataset of $N_{ds} = 10^5$ independent samples. Wand split it into training set with 90000 samples and test set

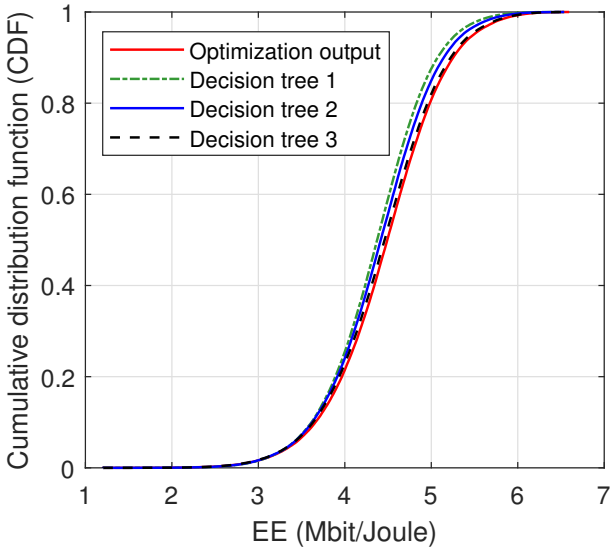


Fig. 3: Performance comparison of the decision tree models with the traditional optimization output.

Table II: Architecture of DNN model 1 with 9,341 trainable parameters.

	Size	Parameters	Activation function
Input	216		
Layer 1 (Dense)	26	5642	elu
Layer 2 (Dense)	35	945	elu
Layer 3 (Dense)	30	1080	elu
Layer 4 (Dense)	30	930	elu
Layer 5 (Dense)	24	744	linear

of 10000 samples. For each of the sample, we have obtained optimal power allocation using traditional optimization algorithms proposed in [12]. Out of the training data 90% of the samples were used for training and 10% samples are used for validation. We have used mean square error (MSE) as the loss function and employed Adam optimizer [14]. The choice of loss function was done after testing different loss functions.

Deep Learning: Figure 2 compares the performance of two DNN models, which estimates the power allocation vector, with that of the traditional optimization technique. It plots the cumulative distribution function (CDF) of the EE obtained for different locations of secondary and primary UEs. Each of the secondary AP employs MR precoding based on the estimated channel gains and applies power allocation vector

Table III: Architecture of DNN model 2 with 50,584 trainable parameters.

	Size	Parameters	Activation function
Input	216		
Layer 1 (Dense)	100	21700	relu
Layer 2 (Dense)	100	10100	relu
Layer 3 (Dense)	80	8080	elu
Layer 4 (Dense)	80	6480	relu
Layer 5 (Dense)	40	3240	relu
Layer 6 (Dense)	24	984	linear

Authorized licensed use limited to: INDIAN INSTITUTE OF TECHNOLOGY GUWAHATI. Downloaded on June 06,2023 at 07:45:14 UTC from IEEE Xplore. Restrictions apply.

Table IV: Parameters of the decision trees.

	Depth	Leaf nodes	MAE
Decision tree 1	18	30000	5.7×10^{-4}
Decision tree 2	25	50000	3.9×10^{-4}
Decision tree 3	30	90000	1.2×10^{-4}

received from the CPU. The DNN architecture of the model 1, which has 9341 trainable parameters, is given in Table II. The performance metric of average mean absolute error (MAE) obtained with this model is 6.22×10^{-4}. We see that the DNN model 1 tracks the CDF of the optimization output well and is very close to it for smaller values of EE. To further improve the DNN performance we have also trained another model with 50584 trainable parameters. Its architecture is shown in Table III. As expected, it performs better than the model 1 with slightly more complexity as it has more neurons in the hidden layers. It is able to achieve a lower MAE of 4.5×10^{-4}. We have tuned the values for learning rate, batch size, and the number of epochs to improve the performance. For both models, we have used a learning rate of 10^{-4}, batch size of 100, and trained the models for 200 epochs. We have used python library Keras to train these models.

Decision Trees: Figure 3 compares the performance of three decision trees. It plots the CDF of the EE achieved by the decision trees along with the CDF of the traditional optimization technique. We have used sklearn python library to train the decision tree. We did trail and error on different parameters of the decision trees in sklearn. We have used squared error criterion to get variance reduction as the feature selection criterion. We have chosen best split strategy. Main parameters and corresponding MAE values of the three decision trees are given in Table IV. We see that the MAE decreases as the depth of the tree increases and performance improves. We see that the decision tree 3 performs close to the traditional optimization based approaches. Therefore, decision trees based regression can yield good performance with much smaller training time.

VI. Conclusion

In this paper, we developed different machine learning models that estimate the EE maximization power allocation of an average interference constrained secondary cell-free network. We showed that DNNs perform close to the traditional optimization techniques while requiring much lower number of computations. We also saw that the decision tree based model can perform very close to the optimal. Therefore, energy and spectrum efficient power allocation can be performed by the machine learning models with reasonably good accuracy with lower complexity.

Acknowledgement

Authors would like to thank Zakir Hussain Shaik and Erik G. Larsson from Department of Electrical Engineering (ISY), Linköping University, Linköping, Sweden, for valuable discussions and sharing the Matlab code.

References

[1] H. Q. Ngo, A. Ashikhmin, H. Yang, E. G. Larsson, and T. L. Marzetta, "Cell-free massive MIMO versus small cells," *IEEE Transactions on Wireless Communications*, vol. 16, no. 3, pp. 1834–1850, March 2017.

[2] G. Interdonato, E. Björnson, H. Q. Ngo, P. Frenger, and E. G. Larsson, "Ubiquitous cell-free massive MIMO communications," *EURASIP Journal on Wireless Communications and Networking*, vol. 2019, no. 1, p. 197, 2019.

[3] D. L. Galappaththige and G. A. A. Baduge, "Exploiting underlay spectrum sharing in cell-free massive MIMO systems," *IEEE Transactions on Communications*, pp. 1–1, 2021.

[4] F. Rezaei, C. Tellambura, and A. Tadaion, "Rate enhancement for distributed massive MIMO systems with underlay spectrum sharing," in *Proc. of IEEE Vehicular Technology Conference (VTC2020-Fall)*, Nov 2020, pp. 1–5.

[5] F. Rezaei, A. R. Heidarpour, C. Tellambura, and A. Tadaion, "Underlaid spectrum sharing for cell-free massive MIMO-NOMA," *IEEE Communications Letters*, vol. 24, no. 4, pp. 907–911, 2020.

[6] E. Au, "Ieee 802.11 be: Extremely high throughput [standards]," *IEEE Vehicular Technology Magazine*, vol. 14, no. 3, pp. 138–140, 2019.

[7] Federal Communications Commission (FCC), "Amendment of the commission's rules with regard to commercial operations in the 3550-3650 MHz band," Tech. Rep. FCC-15-47, Feb. 2015.

[8] ——, "Unlicensed use of the 6 GHz band; Expanding flexible use in mid-band spectrum between 3.7 and 24 GHz," Tech. Rep. FCC-20-51, 2020.

[9] M. El Tanab and W. Hamouda, "Resource allocation for underlay cognitive radio networks: A survey," *IEEE Communications Surveys Tutorials*, vol. 19, no. 2, pp. 1249–1276, 2017.

[10] M. Alonzo, S. Buzzi, A. Zappone, and C. D'Elia, "Energy-efficient power control in cell-free and user-centric massive MIMO at millimeter wave," *IEEE Transactions on Green Communications and Networking*, vol. 3, no. 3, pp. 651–663, 2019.

[11] H. Q. Ngo, L.-N. Tran, T. Q. Duong, M. Matthaiou, and E. G. Larsson, "On the total energy efficiency of cell-free massive MIMO," *IEEE Transactions on Green Communications and Networking*, vol. 2, no. 1, pp. 25–39, 2018.

[12] Z. H. Shaik, R. Sarvendranath, and E. G. Larsson, "Energy-efficient power allocation for an underlay spectrum sharing radioweaves network," in *Proc. ICC*, May 2022, pp. 799–804.

[13] L. Sanguinetti, A. Zappone, and M. Debbah, "Deep learning power allocation in massive MIMO," in *Proc. Asilomar Conf. on Signals, Syst., and Comput.*, Oct. 2018, pp. 1257–1261.

[14] Y. Zhao, I. G. Niemegeers, and S. H. De Groot, "Power allocation in cell-free massive mimo: A deep learning method," *IEEE Access*, vol. 8, pp. 87 185–87 200, May 2020.

[15] N. Rajapaksha, K. B. Shashika Manosha, N. Rajatheva, and M. Latva-Aho, "Deep learning-based power control for cell-free massive MIMO networks," in *Proc. ICC*, Jun. 2021, pp. 1–7.

[16] M. Zaher, Ö. T. Demir, E. Björnson, and M. Petrova, "Learning-based downlink power allocation in cell-free massive MIMO systems," *IEEE Trans. Wireless Commun.*, pp. 1–1, Jul. 2022.

[17] R. Sarvendranath and N. B. Mehta, "Antenna selection with power adaptation in interference-constrained cognitive radios," *IEEE Trans. Commun.*, vol. 62, no. 3, pp. 786–796, Mar. 2014.

[18] Ö. T. Demir, E. Björnson, and L. Sanguinetti, "Foundations of user-centric cell-free massive MIMO," *Foundations and Trends in Signal Processing*, vol. 14, no. 3-4, pp. 162–472, 2021.

[19] T. L. Marzetta, E. G. Larsson, H. Yang, and H. Q. Ngo, *Fundamentals of Massive MIMO*. Cambridge University Press, 2016.

[20] I. J. Goodfellow, Y. Bengio, and A. Courville, *Deep Learning*. Cambridge, MA, USA: MIT Press, 2016, http://www.deeplearningbook.org.

[21] M. Mohri, A. Rostamizadeh, and A. Talwalkar, *Foundations of Machine Learning*. MIT Press, 2012.

Authorized licensed use limited to: INDIAN INSTITUTE OF TECHNOLOGY GUWAHATI. Downloaded on June 06,2023 at 07:45:14 UTC from IEEE Xplore. Restrictions apply.